Comparison of fenofibrate – mesoporous silica drug-loading processes for enhanced drug delivery

Robert J. Ahern[1], John P. Hanrahan[2], Joseph M. Tobin[2], Katie B. Ryan[1] and Abina M. Crean[1, *]

[1]School of Pharmacy, University College Cork, Ireland,

[2]Glantreo Ltd, Environmental Research Institute, University College Cork, Ireland,

[*]Corresponding Author, Address: The Cavanagh Pharmacy Building, School of Pharmacy, College Road, University College Cork, Ireland,

Telephone: +353 (0) 214901667, Email Address: a.crean@ucc.ie

Abstract

Loading a poorly water-soluble drug onto a high surface area carrier such as mesoporous silica (SBA-15) can increase the drug's dissolution rate and oral bioavailability. The loading method can influence subsequent drug properties including solid state structure and release rate. The objective of this research was to compare several loading processes in terms of drug distribution, solid state form and drug release properties. A model poorly water-soluble drug fenofibrate was loaded onto SBA-15 using; (i) physical mixing, (ii) melt, (iii) solvent impregnation, (iv) liquid CO_2 and (v) supercritical CO_2 methods. Physical mixing resulted in heterogeneous drug-loading, with no evidence of drug in the mesopores and the retention of the drug in its crystalline state. The other loading processes yielded more homogeneous drug-loading, the drug was deposited into the mesopores of the SBA-15 and was non-crystalline.. All the processing methods resulted in enhanced drug release compared to the unprocessed drug with the impregnation, liquid and SC-CO_2 producing the greatest increase at t=30 min.

Keywords: SBA-15, fenofibrate, supercritical CO_2, poorly water-soluble, amorphous, drug-loading, mesoporous silica, drug release

1.0 Introduction

It has been long established that increasing the effective surface area of a poorly water-soluble drug in contact with the dissolution medium can enhance drug dissolution (Bruner, 1904, Nernst, 1904). This can be achieved by loading drug on silica-based ordered mesoporous materials (OMMs) which are characterised by high surface areas, large pore volumes, narrow pore size distributions (5 – 8 nm) and ordered unidirectional pore networks. These properties allow for homogeneous and reproducible drug-loading and release (Manzano et al., 2009, Vallet-Regi et al., 2007, Vallet-Regi et al., 2001).

Many publications have focussed on understanding the key properties of OMMs that influence drug-loading and dissolution rate enhancement. It has been reported that the surface area determines how much drug can be loaded onto OMMs and OMM particle size has an impact on drug release rate, with larger silica particles resulting in slower drug release because of the longer mesopore length (Chen et al., 2012). The pore volume influences the amount of drug loaded, especially if the drug is dissolved in a solvent that can carry it into the mesopores (Vallet-Regi et al., 2007). Larger pore sizes encourage greater drug release rates (Horcajada et al., 2004), while pore geometry has also be shown to affect drug-loading and release (Izquierdo-Barba et al., 2005). Stabilisation of amorphous drug for up to 12 months has also been ascribed to the mesopores of the OMM (Mellaerts et al., 2010, Shen et al., 2010). The silica surface can be functionalised with organic groups to encourage greater

46 drug-loading by creating stronger bonding between the silica surface and drug (Manzano et
47 al., 2008), and to extend drug release (Vallet-Regi et al., 2007).
48 Despite the body of literature evaluating the different properties of OMM affecting drug-
49 loading and release, there seems to be a lack of clarity regarding the optimum processing
50 method to load drug onto the OMM and the subsequent implications for drug delivery.
51 Various loading methods have been employed including physical mixing (Song et al., 2005,
52 Qian and Bogner, 2011), solvent based methods that either involve the suspension of the
53 OMM in a drug-solvent solution (Andersson et al., 2004, Izquierdo-Barba et al., 2005,
54 Charnay et al., 2004) or impregnation of the OMM by dropwise addition of a concentrated
55 drug solution (Mellaerts et al., 2008a, Van-Speybroeck et al., 2008). Some researchers have
56 mixed the drug and silica and heated the resultant mixture to below (Tozuka et al., 2005) or
57 above the drug's melting point (Aerts et al., 2010, Mellaerts et al., 2008a, Shen et al., 2010).
58 Alternative loading methods such as supercritical CO_2 (SC-CO_2) (Ahern et al., 2012,
59 Sanganwar and Gupta, 2008) have also been proposed to load drug onto OMMs. The high
60 densities of liquid and SC-CO_2 should permit a large amount of drug to be solubilised, while
61 the high diffusivity of the SC-CO_2 should facilitate ready access to the mesopore network
62 (Fages et al., 2004, Pasquali and Bettini, 2008, York, 1999).
63 To our knowledge this is the first study to directly compare physical mixing, melt, solvent
64 impregnation and CO_2 based drug-loading methods in terms of the subsequent impact on drug
65 – OMM properties, in particular drug distribution, solid state properties and drug release. To
66 our knowledge, this is also the first study to enhance drug dissolution by loading drug onto
67 OMM using a liquid (near-critical) CO_2 loading method. The model OMM in this study was
68 SBA-15 and fenofibrate was employed as a representative Class II drug as defined by the
69 biopharmaceutics classification system (BCS) (Amidon et al., 1995). It is highly lipophilic

(log P = 5.3) (Wishart et al., 2008) and practically insoluble in water (< 0.8 µg/ml) (Jamzad and Fassihi, 2006).

2.0 Materials and methods

2.1 Materials

Fenofibrate was supplied by Kemprotec Ltd. (United Kingdom). CO_2 was supplied by Irish Oxygen Ltd. (Ireland). Hydrochloric acid (HCl), dichloromethane (DCM), potassium bromide (KBr), phencyclidine hydrochloride (P-123) and tetraethyl orthosilicate (TEOS) were supplied by Sigma-Aldrich Ltd. (Ireland). Sodium dodecyl sulphate (SDS) was supplied by Fisher Scientific Ltd. (Ireland).

2.1.1 Preparation of SBA-15

SBA-15 was synthesized according to the method outlined in literature (Zhao et al., 1998). Briefly, 200 g of tri-block polymer (P123) was dissolved in 1.6 M HCl solution and was heated to 40 ^{o}C to completely dissolve the polymer, after which 607 ml of 98% TEOS was added to the solution. The solution was stirred for 24 h at 40 ^{o}C and dried for a further 96 h at 60 ^{o}C. The SBA-15 was recovered by filtration, washed with deionised water to remove any remaining ethanol and HCl, prior to calcination at 550 ^{o}C for 14 h to remove the polymer template.

2.2 Drug-loading methods

Drug-silica samples were prepared with a ratio of 1 mg drug per 3 m^2 mesoporous silica. In each case approximately 400 mg of drug was combined with 2 g mesoporous silica and

processed according to the methods detailed below. All samples were prepared in triplicate. Following preparation, a portion of each drug-silica sample was placed in screw-capped plastic tubes (Sarstedt AG, Germany) and stored in a desiccator at ambient temperatures prior to analysis. The remaining part was stored under accelerated storage conditions at 75% relative humidity (RH) and 40 ^{o}C prior to analysis to assess stability (FDA, 2003).

2.2.1 Physical mixing

Drug-mesoporous silica physical mixes were prepared by blending the drug and SBA-15 for 30 min at 100 revolutions per minute (rpm) using an AR402 Erweka blender (Erweka GmbH, Germany).

2.2.2 Melt method

The melt method involved heating the drug above its melting point (>80 ^{o}C) and relied on its molten viscosity to distribute the drug on the mesoporous silica surface. The drug was manually combined with the mesoporous silica to increase the homogeneity of drug distribution. The sample was maintained above 80 ^{o}C for 24 h using an E-series binder oven (Erweka GmbH, Germany) and thereafter cooled to ambient temperature.

2.2.3 Solvent impregnation

Samples were prepared according to the method reported by Mellaerts and co-workers (Mellaerts et al., 2008a). Approximately 8 ml of a concentrated solution of fenofibrate (50 mg/ml) in DCM was added dropwise to the mesoporous silica; after each addition the powder was intensively ground with a pestle. Thereafter, the sample was dried at 40 ^{o}C for 48 h under vacuum (100 Pa).

2.2.4 Liquid and SC-CO_2 loading

The drug and mesoporous silica were combined in a high-pressure reactor (BC 316), (High Pressure Equipment Company, USA) and stirred using a magnetic stirring. The cell was heated to 25 ^{o}C using heating tape and maintained constant for the duration of the experiment using a temperature monitor (Horst GmbH, Germany). The reactor cell was filled with liquid CO_2. A high pressure pump (D Series Syringe Pump 260D, Teledyne ISCO, USA) was then used to pump additional CO_2 to a final processing pressure (27.58 MPa). At the end of the experiment the cell was depressurised rapidly by venting the CO_2. The SC-CO_2 loading process followed a similar procedure, except that the cell was heated to 40 ^{o}C.

2.3 Physicochemical characterisation

2.3.1 Porosity analysis

Surface area and pore size analysis by nitrogen (N_2) adsorption was carried out using a Gemini VI surface area and pore size analyser, (Micromeritics, USA). The samples were degassed for 24 h at 50 ^{o}C in a FlowPrep 060 sample degas system, (Micromeritics, USA) prior to analysis. During analysis, liquid N_2 at -196 ^{o}C maintained isothermal conditions. The pore volume along with pore width were calculated using the Barrett-Joyner-Halenda (BJH) adsorption correlation (Barrett et al., 1951). Each individual fenofibrate-silica processed sample was analysed in duplicate.

Comparison of the measured pore volume of the drug-silica samples with the theoretical pore volume provides some indication of the location of the drug in the samples. The theoretical pore volume (P.V.) of the processed fenofibrate-silica samples can be determined based on the relative mass fractions of silica and drug present in the sample and their respective pore volumes. As fenofibrate is a non-porous material its pore volume can be ignored and the

theoretical pore volume (P.V.) of the processed fenofibrate-silica samples was calculated according to Eq. 1.

$$\text{Theoretical P.V.} = (\text{P.V.}_{(MS)} \times \text{M}_{(MS)}) \quad (1)$$

$\text{P.V.}_{(MS)}$ refers to the pore volume (cm^3/g) of unprocessed SBA-15. $\text{M}_{(MS)}$ refers to the mass fraction of mesoporous silica in the fenofibrate-silica sample. The mass fraction of drug present in the fenofibrate-silica samples was determined by thermogravimetric analysis (TGA) as described in Section 2.3.2. Eq. 1 was employed based on the assumption that there was no chemical or physical interaction between silica and fenofibrate in the fenofibrate-silica samples.

The percentage difference between the theoretical and measured pore volumes (% ΔPV) was calculated using Eq.2

$$\%\ \Delta PV = ((\text{theoretical P.V.} - \text{measured P.V.}) / \text{theoretical P.V.})*100\% \quad (2)$$

2.3.2 Thermogravimetric analysis

Thermogravimetric analysis (TGA) was carried out using a TGA 500, (TA Instruments Ltd., United Kingdom). Samples in the weight range 2 to 10 mg were loaded onto tared platinum pans and heated from ambient temperature to 900 ^{o}C, at a heating rate of 10 $^{o}C.min^{-1}$ under an inert N_2 atmosphere. All samples were analysed in triplicate. The moisture present in the samples was calculated from the weight loss between ambient temperature and 100 ^{o}C and the drug quantity was calculated from the weight loss between 100 to 900 ^{o}C, corrected for the weight loss over the same temperature range for silica only (Hillerström et al., 2009,

165 Van-Speybroeck et al., 2009). TGA thermograms were analysed using Universal Analysis
166 2000 software, (TA Instruments Ltd., United Kingdom). Drug-loading efficiency was
167 calculated using Eq. 3.
168
169 Drug-loading Efficiency (%) = (actual drug loaded/theoretical drug loaded) x 100% (3)
170
171 The theoretical drug-loading was based on mass fraction of drug and silica used to prepare
172 samples.
173
174 **2.3.3 Differential scanning calorimetry**
175 Differential scanning calorimetry (DSC) was carried out using a DSC Q1000, (TA
176 Instruments Ltd., United Kingdom) operated in modulated mode. DSC was used to measure
177 the glass transition temperature (T_g), melting point (T_m) and enthalpy of melting of
178 fenofibrate and fenofibrate-silica samples. Samples in the weight range 3 to 5 mg were
179 weighed on a MX5 microbalance (Mettler Toledo International Inc., USA) into Tzero
180 aluminium pans (non-hermetic) (TA Instruments Ltd., United Kingdom). The samples were
181 heated from -40 to 120 ^{o}C at a heating rate of 3 ^{o}C.min^{-1} with modulation frequency of 1
182 ^{o}C.min^{-1} every 60 s. An inert atmosphere was maintained using a N_2 flow rate of 50 ml.min^{-1}.
183 A refrigerant cooling system, the RCS 40 (TA Instruments Ltd., United Kingdom) was used
184 to cool samples below ambient temperature. Analysis of DSC thermograms was conducted
185 using Universal Analysis 2000 software, (TA Instruments Ltd., United Kingdom).
186
187
188

189 **2.3.4 Powder X-ray diffraction**

190 Powder x-ray diffraction (pXRD) was performed to determine changes in the solid state
191 structure of fenofibrate after processing with silica. Analysis was performed at ambient
192 temperature using a Stadi MP diffractometer, (Stoe GmbH, Germany) operating in
193 transmission mode with a linear position-sensitive detector, an anode current of 40 mA, an
194 accelerating voltage of 40 kV and Cu Kα1 X-radiation (λ = 1.5406 Å) typically over a scan
195 range of 3.5 to 60 ° 2θ, scanning in steps of 2 ° for 90 s per step. Samples were held between
196 acetate foils during analysis.

197

198 **2.3.5 *In vitro* fenofibrate release**

199 The dissolution and release rates of unprocessed fenofibrate and processed fenofibrate-
200 mesoporous silica samples were measured in a dissolution medium composed of 0.1 M HCl
201 and 0.3% (w/v) SDS under sink conditions at 37 ^{o}C. The dissolution apparatus employed was
202 a USP Type II (paddle method) with a dissolution volume of 900 ml and paddle stirring
203 maintained at 100 rpm. A fixed weight of fenofibrate (15 mg) or a mass of drug-silica sample
204 containing an equivalent mass of drug was added to the dissolution medium. Samples were
205 withdrawn at defined time points and replaced with fresh media to ensure a constant
206 dissolution volume. Samples withdrawn were filtered through a 0.2 µm syringe filter
207 (Sarstedt AG, Germany) prior to analysis by RP-HPLC as described below.

208

209 **2.3.6 RP-HPLC analysis**

210 RP-HPLC analysis was performed using an Agilent 1200 series HPLC system with a UV/VIS
211 detector (Agilent Technologies, USA). A reversed-phase column Kinetex C-18 column (150
212 mm x 4 mm) with internal pore width 2.6µm (Phenomenex Ltd., United Kingdom), a mobile

213 phase of acetronitrile and water (70:30) at a flow rate of 1 ml.min^{-1} and an injection volume
214 of 5 µl were employed. The wavelength for fenofibrate detection was set at 286 nm. The
215 retention time for fenofibrate was 4.5 min.
216

217 3.0 Results

218 3.1 Drug-loading

219 Similar loading efficiencies of greater than 90% were determined for the impregnation, liquid
220 and SC-CO_2 methods, Table 1. Values greater than 100% were determined for the physical
221 and melt samples. However large intra-batch variabilities were evident in these samples that
222 may be attributed to segregation during preparation due to density differences between the
223 mesoporous silica and fenofibrate. In the case of both the physical and melt samples, poor
224 mixing resulted in heterogeneous distribution of drug throughout the silica substrate. The low
225 variability in drug-loading for the impregnation, liquid and SC-CO_2 processed samples was
226 indicative of more homogeneous drug distribution. All loading methods, with the exception
227 of the physical mix, involved the disruption of the drug solid particles by melting or
228 dissolution. For the melt samples, drug distribution was reliant on the viscosity of molten
229 drug and the degree of drug and silica mixing. Drug dissolution in a solvent in the
230 impregnation, liquid and SC-CO_2 samples facilitated more uniform drug distribution in these
231 samples.
232

233 3.2 Porosity analysis

234 Changes in silica porosity after drug-loading can assist in understanding how the drug is
235 distributed throughout the silica sample. Mesoporous silica starting material had a very large

236 pore volume (>0.50 cm^3/g) and displayed the type IV adsorption-desorption isotherm and H1
237 hysteresis loop (Fig.1a) characteristic of mesoporous materials, (Sing et al., 1985). These
238 characteristics were retained post drug-loading (Fig.1), which indicated that silica was still
239 mesoporous. With the exception of the physical mix, all drug loaded samples showed marked
240 reductions in the mesoporous silica pore size and volume. The closure point (P/P_o) of the
241 hysteresis loop was reduced for all samples, with the exception of the physical mix (Fig.1),
242 indicating a reduction in pore sizes (Izquierdo-Barba et al., 2005). The greatest reduction was
243 observed for the sample prepared by the melt method. The pore size distribution in relation to
244 the pore volume for the various samples is shown in Fig 2. Only a slight change in pore size
245 distribution was seen for the physical mix (Fig.2a). Both impregnation and liquid CO2
246 samples show similar reductions in pore size; interestingly the SC-CO_2 sample showed a
247 lower reduction in pore size compared to these samples. The melt sample showed the greatest
248 spread of pore sizes (Fig.2b).
249 The reduction in pore volume (% ΔPV) calculated with Eq.2 were used to quantitatively
250 compare the reductions in pore volumes of the processed samples compared to the theoretical
251 pore volume. The % ΔPV values are shown in Table 1. The % ΔPV of the physical mix was
252 negligible showing that the presence of the drug had little effect on the silica pore volume in
253 these samples. One-way ANOVA followed by the Tukey test showed that all the other
254 samples had a significantly higher % ΔPV compared to the physical mix ($p < 0.05$) indicating
255 that processing by these methods resulted in a reduction in the silica pore volume due to drug
256 deposition into the silica mesopores and blocking of the mesopores. Despite having similar
257 loading efficiencies, impregnation and liquid CO_2 samples had a significantly higher % ΔPV
258 values compared to the SC-CO_2 samples ($p < 0.05$).
259

3.3 Solid state analysis

Powder XRD and DSC analysis of samples was undertaken to determine whether the loading methods resulted in differences in fenofibrate solid state behaviour. The pXRD diffractogram of the fenofibrate crystalline starting material was in accordance with that previously reported (Heinz et al., 2009). The pXRD diffractograms of drug-silica samples, with the exception of the physical mix, showed no peaks indicating that the drug in these samples was in a non-crystalline state (Fig.3).

The melting point for the starting crystalline fenofibrate agreed with the reported T_m of 79 – 81 ^oC (Heinz et al., 2009). Thermal events in the temperature range -20 to -12 ^oC were noted during DSC analysis of the silica starting material (Fig.4a). This behaviour was previously reported as the melting point of frozen water confined in the mesopores of mesoporous silica (Kittaka et al., 2011). Endothermic thermal events in the same range -20 to -12 ^oC were noted in all drug-silica samples regardless of the method of the loading. As fenofibrate's T_g was reported in this temperature region at -20 ^oC, (Heinz et al., 2009) it was not possible to conclusively detect the T_g of amorphous fenofibrate in any of these drug-silica samples.

A large melting endotherm with an onset of 78 ^oC was visible in DSC thermogram of the physical mix, while there was a slight melting endotherm in the melt sample, indicative of the presence of residual crystalline drug (Fig.4b). The absence of melting endotherms in the impregnation, liquid and SC-CO_2 samples (data not shown), supported the pXRD results that the drug was in a non-crystalline state in these samples.

3.4 *In vitro* drug release

The release of drug from the silica carrier is a key performance indicator to consider when employing OMM for drug dissolution enhancement. The *in vitro* release of drug from drug-

284 silica samples and the dissolution of the starting fenofibrate are shown in Figure 5. Utilising
285 mesoporous silica as a carrier material improved the drug dissolution rate for all processed
286 samples. The physical mix showed a slower rate of drug release compared to all of the other
287 loading methods. The release profiles of drug from the impregnation, liquid and SC-CO_2
288 loaded samples were similar according to the difference (f_1) and similarity (f_2) factors (Moore
289 and Flanner, 1996) and the modified difference factor $f_1^{'}$ (Costa and Sousa-Lobo, 2001). Drug
290 was released in a rapid manner in the first 20 min. After 20 min the drug release levelled
291 between 70 – 80 % and did not increase between 20 and 120 min. The release from the melt
292 sample was different in nature to the impregnation, liquid and SC-CO_2 samples according to
293 the f_1, modified $f_1^{'}$, and f_2 values. One-way ANOVA followed by the Tukey test at each
294 individual time point showed significant differences between the physical and melt release
295 profiles from 5 to 20 min compared to the other samples. After 30 min, the melt release was
296 not significantly different to the impregnation, liquid and SC-CO_2 samples release, according
297 to one-way ANOVA. The physical mix had a significantly less release across all time points
298 ($p < 0.05$).
299 In the case of physical mix and melt samples, the variability in drug release at each time point
300 was high in contrast to the other samples reflecting the heterogeneous drug-loading in these
301 samples referred to previously in Section 3.1. The similarity of the drug release profiles for
302 the melt, impregnation, liquid and SC-CO_2 samples indicated that the deposition behaviour of
303 drug in the mesopores did not affect its release.
304

305 ## 3.5 Stability analysis

306 The presence of amorphous drug in the processed samples potentially posed a risk to the drug
307 solid state stability of these formulations. Recrystallization of unstable amorphous forms can

adversely affect drug properties such as dissolution performance. The solubility and dissolution enhancement associated with the amorphous form (Hancock and Parks, 2000) can be lost if there is re-crystallisation occurs While it has been reported that the OMMs can stabilise non-crystalline drug forms (Mellaerts et al., 2010, Shen et al., 2010), the influence of loading method on stability has not been reported. After 12 months accelerated storage at 40 ^{o}C and 75% RH, there was no evidence of re-crystallisation of the amorphous drug in the pXRD diffractograms of the melt, impregnation, liquid and SC-CO_2 samples (Fig.6). Interestingly, the pore volume of the physical mix sample post storage was reduced compared to the as prepared sample; a significant increase ($p < 0.05$) in % ΔPV was determined (Table 1) according to one-way ANOVA followed by the Tukey test. The reduction of the pore volume was evident in the decrease of size of the larger pores size (Fig.7). The pore volume and size of the melt, impregnation liquid and SC-CO_2 samples remained unchanged post 1 month storage.

After storage for 1 month, there was some improvement in drug release from the physical mix samples (Fig.8); the f_1, modified $f_1^{'}$, and f_2 values showed a difference between the profiles. One-way ANOVA analysis followed by the Tukey test across each time point showed a significant increase in drug release post storage compared to the as prepared sample ($p < 0.05$). Long term storage for up to 12 months did not enhance the drug release rate of the drug in the impregnation, liquid and SC-O_2 samples (data not shown).

4.0 Discussion

The results of this work highlight the influence of the loading process employed on drug distribution on the mesoporous silica structure. The physical mixing and melt methods

331 employed resulted in heterogeneous distribution of drug throughout the MESOPOROUS
332 SILICA due to blending difficulties arising from differences in density between the drug and
333 silica. The impregnation, liquid and SC-CO_2 methods obtained samples with drug
334 homogeneously dispersed throughout the mesoporous silica surfaces similar to that reported
335 previously (Ahern et al., 2012, Van-Speybroeck et al., 2009). This was facilitated by
336 dissolution/ of the drug in the solvent.
337 Changes in the porosity of silica post processing also highlighted differences in drug
338 distribution resulting from different loading methods. For all loading methods examined, the
339 mesoporous silica retained its type IV adsorption isotherm indicative of its mesoporous
340 nature. Similar findings have been reported previously (Mellaerts et al., 2008b, Morere et al.,
341 2012, Moritz and Laniecki, 2012). The deposition of the drug molecules inside the
342 mesoporous silica mesopores resulted in some of the pores being fully or partially filled with
343 drug molecules, which prevented the adsorption and condensation of the N_2 molecules in the
344 mesopores during subsequent pore volume measurement. Ukmar and co-workers reported
345 that indomethacin loaded onto MCM-41 and SBA-15 using a solvent impregnation method
346 formed a condensed phase that could block passage of the mesopore channels (Ukmar et al.,
347 2011).
348 The melt method resulted in the greatest reduction in pore size and largest reduction in pore
349 volume. This behaviour was attributed to the molten viscosity of drug preventing deep
350 penetration of the mesopores and causing blockage of mesopores. Mellaerts and co-workers
351 utilised a melt method to load itraconazole and ibuprofen onto SBA-15; the subsequent
352 itraconazole–SBA-15 surface area, pore volume and size were similar to the SBA-15, while
353 for ibuprofen-SBA-15 the surface area, pore volume and size were reduced (Mellaerts et al.,
354 2008a). Therefore, the distribution of drug in samples prepared using melt methods is

355 strongly dependent on the drug's molten viscosity, while the ability to form a homogeneous
356 mixture of drug and silica prior to the melting step of the process depends on the density of
357 the powders and method of blending. The decrease in pore size observed was evidence of the
358 drug coating/lining the inside of the mesopores and was also observed by Mellaerts and co-
359 workers (Mellaerts et al., 2008a).
360 Due to the greater diffusivity and extremely low surface tension of SC-CO_2 compared to
361 solvents in a liquid state, there appears to be deeper drug penetration of the silica (Belhadj-
362 Ahmed et al., 2009). This is reflected in the lower reduction of pore volume and pore size
363 observed for the SC-CO_2 samples compared to the impregnation and liquid CO_2 samples,
364 despite all samples having similar drug-loading. From these data it appears that although the
365 drug deposition causes a narrowing of the pore network, it does not preclude N_2 access during
366 measurement to the same extent as in the melt, impregnation and liquid CO_2 samples. It was
367 previously reported that increasing the amount of drug loaded using SC-CO_2 loading
368 correlated with a reduction in pore volume (Ahern et al., 2012). In this work, it is also
369 apparent that the processing method has an important influence on the distribution of drug
370 and subsequent porosity of samples with similar drug-loading.
371 Loading fenofibrate onto SBA-15 using the impregnation, liquid and SC-CO_2 processes
372 resulted in the drug changing from the crystalline to a non-crystalline state. This is in
373 agreement with previous reports showing the crystalline to non-crystalline transition observed
374 when processing drugs with OMMs (Miura et al., 2010, Nishiwaki et al., 2009, Tozuka et al.,
375 2005, Tozuka et al., 2003). Qian and co-workers demonstrated that crystalline to amorphous
376 transitions occurred in physical mixes of drug and silica via a vapour phase-mediated
377 pathway for drugs with a relatively low vapour pressure (Qian and Bogner, 2011). The
378 physical mixing conditions investigated in this study did not result in any detectable

379 amorphization of fenofibrate, perhaps due to the relatively high vapour pressure of
380 fenofibrate.
381 Azais and co-workers studied the confinement of ibuprofen in MCM-41 mesopores (35 and
382 116 Å) using solid state nuclear magnetic resonance. They reported that the ibuprofen in the
383 mesopores was not in a crystalline or amorphous state at ambient temperature (Azais et al.,
384 2006), and proposed the concept of the drug existing as a molecular dispersion in the silica
385 mesopores. The drug loaded onto SBA-15 by the impregnation, liquid and SC-CO_2 processes
386 appeared to be in a molecularly dispersed state as no T_g or T_m was observed. However as
387 highlighted in Section 3.3 frozen water in the pores of mesoporous silica may have
388 confounded the detection of the T_g for fenofibrate in these samples. In the melt sample, there
389 was a small endotherm detected in the DSC thermogram around the drug's melting point,
390 which would indicate that some of the drug was still crystalline.
391 It has been previously reported that fenofibrate existed in an amorphous state post loading
392 onto silica. Van-Speybroeck and co-workers impregnated SBA-15 with fenofibrate and
393 detected the drug T_g at – 20 ^{o}C, this was ascribed to the higher drug load (higher ratio of drug
394 weight to silica surface area) which promoted drug-drug interactions (Van Speybroeck et al.,
395 2010a). Sanganwar and Gupta reported the presence of residual crystallinity post processing
396 of fenofibrate with aerosil using SC-CO_2 (Sanganwar and Gupta, 2008). However, this may
397 be due to the non-porous nature and hence lower surface area of aerosil and again, a
398 relatively higher drug weight to silica surface area ratio. Other studies of drug-loading SBA-
399 15 using an impregnation process have also reported that the drug was molecularly dispersed
400 as there was no T_g or T_m observed (Mellaerts et al., 2010, Mellaerts et al., 2008a, Van
401 Speybroeck et al., 2010b).

Fenofibrate in melt, impregnation, liquid and SC-CO_2 prepared samples was stabilised in the non-crystalline form after 12 month storage under accelerated storage conditions. Fenofibrate is very unstable in its amorphous form; it has a T_g of -20 ^oC, its recrystallization temperature is 40 ^oC and its reduced temperature scale is 0.6 (Zhou et al., 2002), hence amorphous fenofibrate is difficult to isolate due to its rapid recrystallization at ambient conditions. Therefore the prolonged stability at accelerated storage conditions must be attributed to its co-processing with SBA-15. These results correspond with those published by Mellaerts and co-workers who reported that itraconazole was maintained in the amorphous form for up to 12 months after processing with SBA-15 (Mellaerts et al., 2010). Shen and co-workers published similar findings with respect to ibuprofen co-spray-dried with SBA-15 (Shen et al., 2010). The ability of SBA-15 to stabilise drugs in a non-crystalline state has previously been discussed. Qian and co-workers reported that the enthalpy of adsorption of a compound on mesoporous silica can lower the Gibbs free energy and cause spontaneous phase transformation of the molecule from a crystalline to an amorphous state (Qian and Bogner, 2011). Another important factor to the stabilisation of the amorphous form is the effect of nanoconfinement on drug recrystallization. A drug cannot re-crystallize when the space in which it is confined does not exceed the drug molecule width by at least a factor of 10 (Rengarajan et al., 2008, Sliwinska-Bartkowiak et al., 2001).

There was a limited improvement in drug release rate in the physical mix sample, which was previously reported by Miura and co-workers, when they physically loaded the drug K-832 onto the silica material sylysia 350 (Miura et al., 2010). The drug release from the impregnation, liquid and SC-CO_2 samples was rapid and similar. The enhanced rate of drug release was attributable to the more homogeneous distribution of the drug throughout the silica, which spread the drug through all of the available surface area. It has been long

established that drug release rate can be enhanced by increasing the effective drug surface area in contact with the dissolution medium (Brunauer et al., 1938). The increased wettability of the drug after drug-loading (Wang et al., 2006) and the non-crystalline nature of the drug which has a higher Gibbs free energy compared to the crystalline form (Craig et al., 1999, Yu, 2001) were also contributing factors.

The extent of drug release from the physical sample increased after 1 month storage. It has been proposed that water may react with mesoporous silica during storage which causes an increase in the extent of drug release. Itraconazole loaded on mesoporous silica prepared using a solvent impregnation method and stored at 25°C and 97 % RH showed an increase in the extent of drug dissolution post storage (Mellaerts et al., 2010). In this work, the extent of drug release did not improve post 12 months storage for the solvent impregnation, liquid and SC-CO_2 samples. Similar findings were presented by Shen and co-workers who subjected a co-spray dried ibuprofen / SBA-15 sample to 12 month, storage at 40 ^{o}C and 75% RH (Shen et al., 2010). The influence of moisture uptake on the release of drugs loaded on mesoporous silica appears to vary with the loading method and warrants further investigations.

5.0 Summary

The method of loading drug onto SBA-15 was shown to influence drug distribution which is evident by the differences in pore size and volume observed for the samples prepared. With the exception of the physical mix and melt samples, solid state and release properties were similar for all processed samples. All processing methods except the physical mix sample, loaded fenofibrate into the SBA-15 mesopores where it was stabilised in a non-crystalline state for 12 month at 75% RH and 40 ^{o}C. Drug release rates were increased for all samples,

449 but depended on loading method. While different loading methods may result in differences
450 in drug distribution these differences were not shown to result in differences in solid state
451 stability or drug release in the case of the impregnation, liquid and SC-CO_2 processed
452 samples.
453

454 Acknowledgements

455 The authors wish to acknowledge the contribution of Ms. Nuala Maguire for performing the
456 pXRD experiments. This research received financial support from Science Foundation
457 Ireland through the Solid state Pharmaceutical Cluster under grant number 07/SRC/B1158.
458

459 References

460 AERTS, C. A., VERRAEDT, E., DEPLA, A., FOLLENS, L., FROYEN, L., VAN
461 HUMBEECK, J., AUGUSTIJNS, P., VAN DEN MOOTER, G., MELLAERTS, R.
462 and MARTENS, J. A. (2010) Potential of amorphous microporous silica for ibuprofen
463 controlled release. *International Journal of Pharmaceutics,* 397**,** 84-91.
464 AHERN, R. J., CREAN, A. M. and RYAN, K. B. (2012) The influence of supercritical
465 carbon dioxide (SC-CO2) processing conditions on drug loading and physicochemical
466 properties. *International Journal of Pharmaceutics,* 439**,** 92-99.
467 AMIDON, G. L., LENNERNÄS, H., SHAH, V. P. and CRISON, J. R. (1995) A Theoretical
468 basis for a biopharmaceutic drug classification: The correlation of *in vitro* drug
469 product dissolution and *in vivo* bioavailability. *Pharmaceutical Research,* 12**,** 413-
470 420.
471 ANDERSSON, J., ROSENHOLM, J., AREVA, S. and LINDEN, M. (2004) Influences of
472 material characteristics on ibuprofen drug loading and release profiles from ordered
473 micro- and-mesoporous silica matrices. *Chemistry of Materials,* 16**,** 4160-4167.
474 AZAIS, T., TOURNE-PETEILH, C., AUSSENAC, F., BACCILE, N., COELHO, C.,
475 DEVOISSELLE, J.-M. and BABONNEAU, F. (2006) Solid-State NMR Study of
476 Ibuprofen Confined in MCM-41 Material. *Chem Mater,* 18**,** 6382-6390.
477 BARRETT, E. P., JOYNER, L. G. and HALENDA, P. P. (1951) The Determination of pore
478 volume and area distributions in porous substances. I. Computations from nitrogen
479 isotherms. *Journal of the American Chemical Society,* 73**,** 373-380.
480 BELHADJ-AHMED, F., BADENS, E., LLEWELLYN, P., DENOYEL, R. and CHARBIT,
481 G. (2009) Impregnation of vitamin E acetate on silica mesoporous phases using
482 supercritical carbon dioxide. *The Journal of Supercritical Fluids,* 51**,** 278-286.

BRUNAUER, S., EMMETT, P. H. and TELLER, E. (1938) Adsorption of gases in multimolecular layers. *Journal of the American Chemical Society,* 60**,** 309-319.
BRUNER, E. (1904) Reaktionsgeschwindigkeit in heterogenen Systemen. *Z. Phys. Chem.,* 43**,** 56–102.
CHARNAY, C., BEGU, S., TOURNE-PETEILH, C., NICOLE, L., LERNER, D. A. and DEVOISSELLE, J. M. (2004) Inclusion of ibuprofen in mesoporous templated silica: Drug loading and release property. *European Journal of Pharmaceutics and Biopharmaceutics,* 57**,** 533-540.
CHEN, Z., LI, X., HE, H., REN, Z., LIU, Y., WANG, J., LI, Z., SHEN, G. and HAN, G. (2012) Mesoporous silica nanoparticles with manipulated microstructures for drug delivery. *Colloids and Surfaces B: Biointerfaces,* 95**,** 274-278.
COSTA, P. and SOUSA-LOBO, J. M. (2001) Modelling and comparison of dissolution profiles. *European Journal of Pharmaceutical Sciences,* 13**,** 123-133.
CRAIG, D. Q. M., ROYALL, P. G., KETT, V. L. and HOPTON, M. L. (1999) The relevance of the amorphous state to pharmaceutical dosage forms: glassy drugs and freeze dried systems. *International Journal of Pharmaceutics,* 179**,** 179-207.
FAGES, J., LOCHARD, H., LETOURNEAU, J.-J., SAUCEAU, M. and RODIER, E. (2004) Particle generation for pharmaceutical applications using supercritical fluid technology. *Powder Technology,* 141**,** 219-226.
FDA (2003) Guidance for Industry Q1A(R2) Stability Testing of New Drug Substances and Products. IN SERVICES, U. S. D. O. H. A. H. (Ed.), U.S. Department of Health and Human Services.
HANCOCK, B. C. and PARKS, M. (2000) What is the true solubility advantage for amorphous pharmaceuticals? *Pharmaceutical Research,* 17**,** 397-404.
HEINZ, A., GORDON, K. C., MCGOVERIN, C. M., RADES, T. and STRACHAN, C. J. (2009) Understanding the solid-state forms of fenofibrate - A spectroscopic and computational study. *European Journal of Pharmaceutics and Biopharmaceutics,* 71**,** 100-108.
HILLERSTRÖM, A., STAMB, J. V. and ANDERSSONA, M. (2009) Ibuprofen loading into mesostructured silica using liquid carbon dioxide as a solvent. *Green Chemistry,* 11**,** 662-667.
HORCAJADA, P., RAMILA, A., PEREZ-PARIENTE, J. and VALLET-REGI, M. (2004) Influence of pore size of MCM-41 matrices on drug delivery rate. *Microporous and Mesoporous Materials,* 68**,** 105-109.
IZQUIERDO-BARBA, I., MARTINEZ, A., DOADRIO, A. L., PEREZ-PARIENTE, J. and VALLET-REGI, M. (2005) Release evaluation of drugs from ordered three-dimensional silica structures. *European Journal of Pharmaceutical Sciences,* 26**,** 365-373.
JAMZAD, S. and FASSIHI, R. (2006) Role of surfactant and pH on dissolution properties of fenofibrate and dlipizide — A technical note. *AAPS PharmSciTech,* 7.
KITTAKA, S., UEDA, Y., FUJISAKI, F., IIYAMA, T. and YAMAGUCHI, T. (2011) Mechanism of freezing of water in contact with mesoporous silicas MCM-41, SBA-15 and SBA-16: role of boundary water of pore outlets in freezing. *Physical Chemistry Chemical Physics,* 13**,** 17222-17233.
MANZANO, M., AINA, V., AREÁN, C. O., BALAS, F., CAUDA, V., COLILLA, M., DELGADO, M. R. and VALLET-REGÍ, M. (2008) Studies on MCM-41 mesoporous

529 silica for drug delivery: Effect of particle morphology and amine functionalization.
530 *Chemical Engineering Journal,* 137**,** 30-37.
531 MANZANO, M., COLILLA, M. and VALLET-REGI, M. (2009) Drug delivery from ordered
532 mesoporous matrices. *Expert Opinion on Drug Delivery,* 6**,** 1383-1400.
533 MELLAERTS, R., HOUTHOOFD, K., ELEN, K., CHEN, H., VAN SPEYBROECK, M.,
534 VAN HUMBEECK, J., AUGUSTIJNS, P., MULLENS, J., VAN DEN MOOTER, G.
535 and MARTENS, J. A. (2010) Aging behaviour of pharmaceutical formulations of
536 itraconazole on SBA-15 ordered mesoporous silica carrier material. *Microporous and*
537 *Mesoporous Materials,* 130**,** 154-161.
538 MELLAERTS, R., JAMMAER, J. A. G., VAN SPEYBROECK, M., CHEN, H.,
539 HUMBEECK, J. V., AUGUSTIJNS, P., VAN DEN MOOTER, G. and MARTENS,
540 J. A. (2008a) Physical state of poorly water-soluble therapeutic molecules, loaded into
541 SBA-15 ordered mesoporous silica carriers: A case study with itraconazole and
542 ibuprofen. *Langmuir,* 24**,** 8651-8659.
543 MELLAERTS, R., MOLS, R., JAMMAER, J. A. G., AERTS, C. A., ANNAERT, P., VAN
544 HUMBEECK, J., VAN DEN MOOTER, G., AUGUSTIJNS, P. and MARTENS, J.
545 A. (2008b) Increasing the oral bioavailability of the poorly water soluble drug
546 itraconazole with ordered mesoporous silica. *European Journal of Pharmaceutics and*
547 *Biopharmaceutics,* 69**,** 223-230.
548 MIURA, H., KANEBAKO, M., SHIRAI, H., NAKAO, H., INAGI, T. and TERADA, K.
549 (2010) Enhancement of dissolution rate and oral absorption of a poorly water-soluble
550 drug, K-832, by adsorption onto porous silica using supercritical carbon dioxide.
551 *European Journal of Pharmaceutics and Biopharmaceutics,* 76**,** 215-221.
552 MOORE, J. W. and FLANNER, H. H. (1996) Mathematical comparison of dissolution
553 profiles. *Pharm Tech,* 20**,** 64-74.
554 MORERE, J., TENORIO, M. J., TORRALVO, M. J., PANDO, C., RENUNCIO, J. A. R. and
555 CABANAS, A. (2012) Deposition of Pd into mesoporous silica SBA-15 using
556 supercritical carbon dioxide. *The Journal of Supercritical Fluids,* 56**,** 213-222.
557 MORITZ, M. and LANIECKI, M. (2012) Application of SBA-15 mesoporous material as the
558 carrier for drug formulation systems. Papaverine hydrochloride adsorption and release
559 study. *Powder Technology,* 230**,** 106-111.
560 NERNST, W. (1904) Theorie der Reaktionsgeschwindigkeit in heterogenen Systemen. *Z.*
561 *Phys. Chem.,* 47**,** 52–55.
562 NISHIWAKI, A., WATANABE, A., HIGASHI, K., TOZUKA, Y., MORIBE, K. and
563 YAMAMOTO, K. (2009) Molecular states of prednisolone dispersed in folded sheet
564 mesoporous silica (FSM-16). *International Journal of Pharmaceutics,* 378**,** 17-22.
565 PASQUALI, I. and BETTINI, R. (2008) Are pharmaceutics really going supercritical?
566 *International Journal of Pharmaceutics,* 364**,** 176-187.
567 QIAN, K. K. and BOGNER, R. H. (2011) Spontaneous crystalline-to-amorphous phase
568 transformation of organic or medicinal compounds in the presence of porous media,
569 part 1: Thermodynamics of spontaneous amorphization. *Journal of Pharmaceutical*
570 *Sciences,* 100**,** 2801-2815.
571 RENGARAJAN, G. T., ENKE, D., STEINHART, M. and BEINER, M. (2008) Stabilization
572 of the amorphous state of pharmaceuticals in nanopores. *Journal of Materials*
573 *Chemistry,* 18**,** 2537-2539.

SANGANWAR, G. P. and GUPTA, R. B. (2008) Dissolution-rate enhancement of fenofibrate by adsorption onto silica using supercritical carbon dioxide. *International Journal of Pharmaceutics*, 213-218.

SHEN, S.-C., NG, W. K., CHIA, L., DONG, Y.-C. and TAN, R. B. H. (2010) Stabilized amorphous state of ibuprofen by co-spray drying with mesoporous SBA-15 to enhance dissolution properties. *Journal of Pharmaceutical Sciences,* 99, 1997-2007.

SING, K. S. W., EVERETT, D. H., HAUL, R. A. W., MOSCOU, L., PIEROTTI, R. A., ROUQUEROL, J. and SIEMIENIEWSKA, T. (1985) Reporting physisorption data for gas/solid systems with special reference to the determination of surface area and porosity. *Pure Applied Chemistry,* 57, 603-619.

SLIWINSKA-BARTKOWIAK, M., DUDZIAK, G., GRAS, R., SIKORSKI, R., RADHAKRISHNAN, R. and GUBBINS, K. E. (2001) Freezing behaviour in porous glasses and MCM-41. *Colloids and Surfaces A: Physicochemical and Engineering Aspects,* 187-188, 523-529.

SONG, S.-W., HIDAJUT, K. and KAWI, S. (2005) Functionalized SBA-15 materials as carriers for controlled drug delivery: Influence of surface properties on matrix-drug interactions. *Langmuir,* 21, 9568-9575.

TOZUKA, Y., OGUCHI, T. and YAMAMOTO, K. (2003) Adsorption and entrapment of salicylamide molecules into the mesoporous structure of folded sheets mesoporous material (FSM-16). *Pharmaceutical Research,* 20, 926-930.

TOZUKA, Y., WONGMEKIAT, A., KIMURA, K., MORIBE, K., YAMAMURA, S. and YAMAMOTO, K. (2005) Effect of pore size of FSM-16 on the entrapment of flurbiprofen in mesoporous structures. *Chemical and Pharmaceutical Bulletin,* 53, 974-977.

UKMAR, T., GODEC, A., PLANINSEK, O., KAUCIC, V., MALI, G. and GABERSCEK, M. (2011) The phase (trans)formation and physical state of a model drug in mesoscopic confinement. *Phys. Chem. Chem. Phys.,* 13, 16046-16054.

VALLET-REGI, M., BALAS, F. and ARCOS, D. (2007) Mesoporous materials for drug delivery. *Drug Delivery Systems,* 46, 7548-7558.

VALLET-REGI, M., RAMILA, A., DEL REAL, R. P. and PEREZ-PARIENTE, J. (2001) A new property of MCM-41: Drug delivery system. *Chemistry of Materials,* 13, 308-311.

VAN-SPEYBROECK, M., BARILLARO, V., THI, T. D., MELLAERTS, R., MARTENS, J., HUMBEECK, J. V., VERMANT, J., ANNAERT, P., MOOTER, G. V. D. and AUGUSTIJNS, P. (2008) Ordered Mesoporous Silica Material SBA-15: A Broad-Spectrum Formulation Platform for Poorly Soluble Drugs. *Journal of Pharmaceutical Sciences,* 98, 2648-2658.

VAN-SPEYBROECK, M., BARILLARO, V., THI, T. D., MELLAERTS, R., MARTENS, J., HUMBEECK, J. V., VERMANT, J., ANNAERT, P., MOOTER, G. V. D. and AUGUSTIJNS, P. (2009) Ordered Mesoporous Silica Material SBA-15: A Broad-Spectrum Formulation Platform for Poorly Soluble Drugs. *Journal of Pharmaceutical Sciences,* 98, 2648-2658.

VAN SPEYBROECK, M., MELLAERTS, R., MOLS, R., THI, T. D., MARTENS, J. A., VAN HUMBEECK, J., ANNAERT, P., VAN DEN MOOTER, G. and AUGUSTIJNS, P. (2010a) Enhanced absorption of the poorly soluble drug fenofibrate by tuning its release rate from ordered mesoporous silica. *European Journal of Pharmaceutical Sciences,* 41, 623-630.

VAN SPEYBROECK, M., MOLS, R., MELLAERTS, R., THI, T. D., MARTENS, J. A., HUMBEECK, J. V., ANNAERT, P., MOOTER, G. V. D. and AUGUSTIJNS, P. (2010b) Combined use of ordered mesoporous silica and precipitation inhibitors for improved oral absorption of the poorly soluble weak base itraconazole. *European Journal of Pharmaceutics and Biopharmaceutics,* 75**,** 354-365.

WANG, L., CUI, F. D. and SUNADA, H. (2006) Preparation and evaluation of dolid dispersions of nitrendipine prepared with fine silica particles using the melt-mixing method. *Chemical Pharmacy Bulletin,* 54.

WISHART, D., KNOX, C., GUO, A., CHENG, D., SHRIVASTAVA, S., TZUR, D., GAUTAM, B. and MHASSANALI (2008) DrugBank: a knowledgebase for drugs, drug actions and drug targets. *Nucleic Acids Research,* 36.

YORK, P. (1999) Strategies for particle design using supercritical carbon dioxide. *Advanced Drug Delivery Review,* 60**,** 388-398.

YU, L. (2001) Amorphous pharmaceutical solids: Preparation, characterization and stabilization. *Advanced Drug Delivery Review,* 48**,** 27-42.

ZHAO, D., FENG, J., HUO, Q., MELOSH, N., FREDRICKSON, G. H., CHMELKA, B. F. and STUCKY, G. D. (1998) Triblock copolymer synthesis of mesoporous silica with periodic 50 to 300 angstrom pores. *Science* 279**,** 548-552.

ZHOU, D., ZHANG, G. G. Z. and LAW, D. (2002) Physical stability of amorphous pharmaceuticals: Importance of configurational thermodynamic quantities and molecular mobility. *Journal of Pharmaceutical Sciences,* 91.

Supporting Data

Table 1

Comparison of drug-loading efficiency and % ΔPV before and after storage for all processed drug – SBA-15 samples

Processing Method	Loading Efficiency (%) (n = 9)	% ΔPV (n = 6)	% ΔPV, 1 month storage (n = 6)
Physical Mix	106.26 (±42.83)	1.88 (±5.41)	15.29 (±6.08)
Melt Method	103.90 (±30.22)	36.84 (±5.63)	35.09 (±3.89)
Impregnation	92.55 (±5.14)	33.12 (±2.26)	44.40 (±15.92)
Liquid CO_2	93.25 (±5.35)	32.06 (±1.66)	33.68 (±3.66)
SC-CO_2	91.98 (±6.34)	19.64 (±5.30)	21.27 (±4.16)

653 **A** 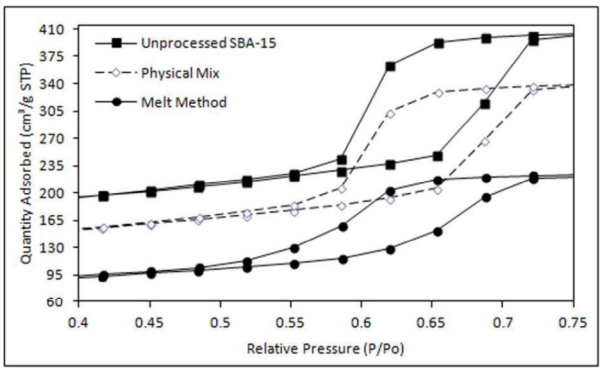

B 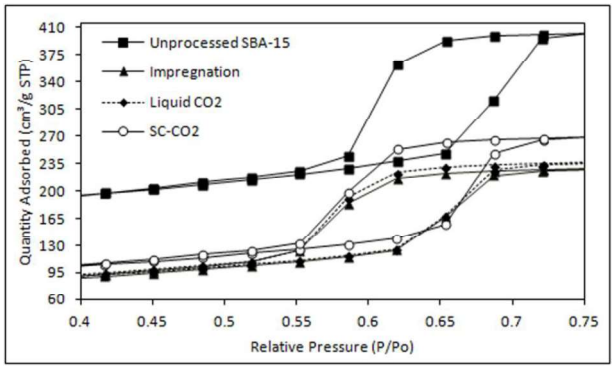

654 **Fig.1** N_2 adsorption/desorption isotherms of (a) unprocessed SBA-15, physical mix and melt method samples and (b) unprocessed SBA-15,

655 impregnation, liquid and SC-CO_2 processed samples.

656

657

658

659

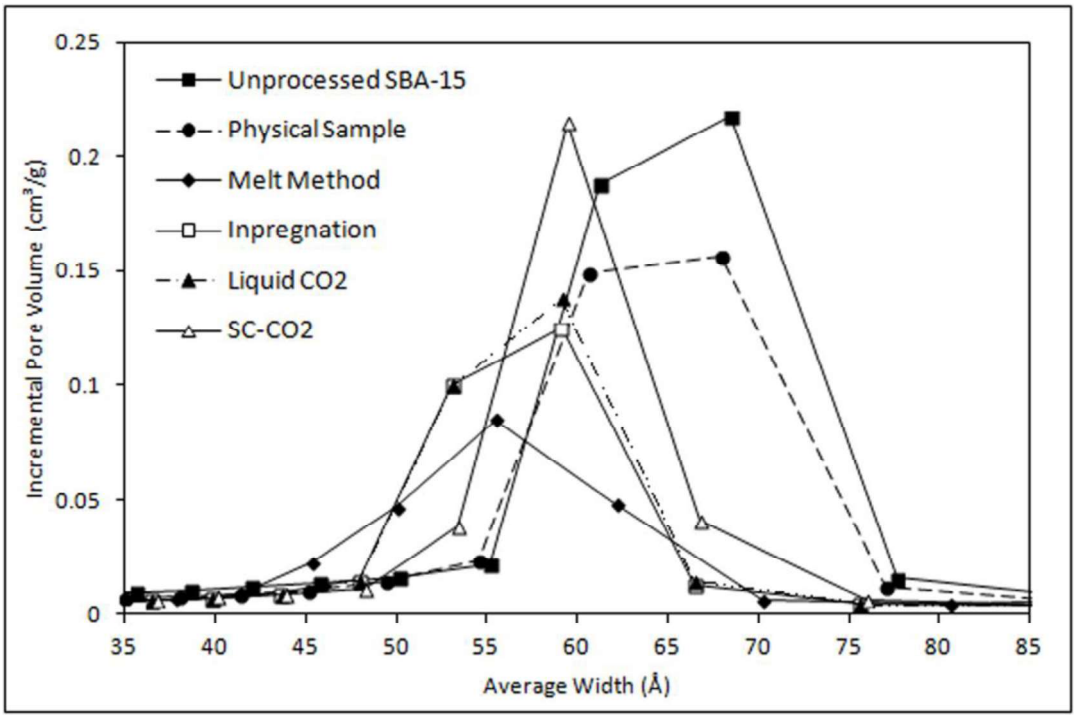

Fig.2: Pore size distribution of unprocessed SBA-15, physical mix, melt, impregnation, liquid and SC-CO_2 processed samples.

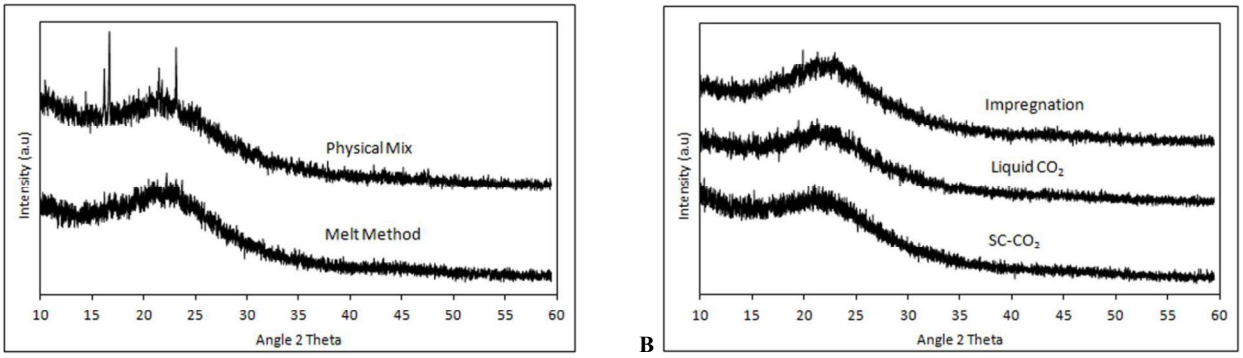

Fig.3 pXRD diffractograms of (a) physical mix and melt method samples and (b) impregnation, liquid and SC-CO_2 processed samples.

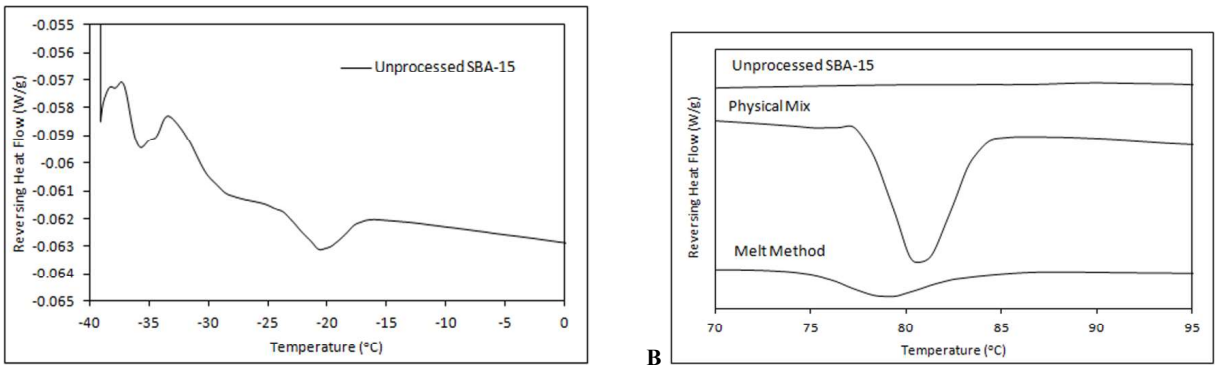

681 **A** **B**

682 **Fig.4** DSC thermograms of (a) unprocessed SBA-15 and (b) physical mix and melt samples with evidence of fenofibrate melting endotherm

683

684 **A** 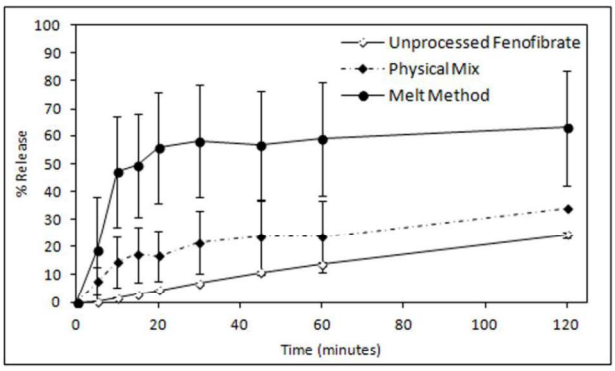

B 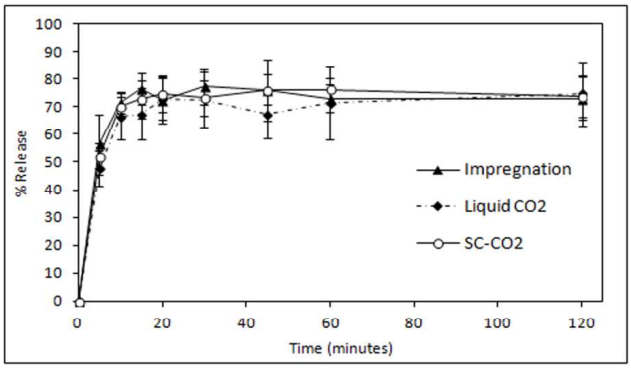

685 **Fig.5** Release profiles of (a) unprocessed fenofibrate, physical mix and melt method samples and (b) impregnation, liquid and SC-CO_2 processed

686 samples

687

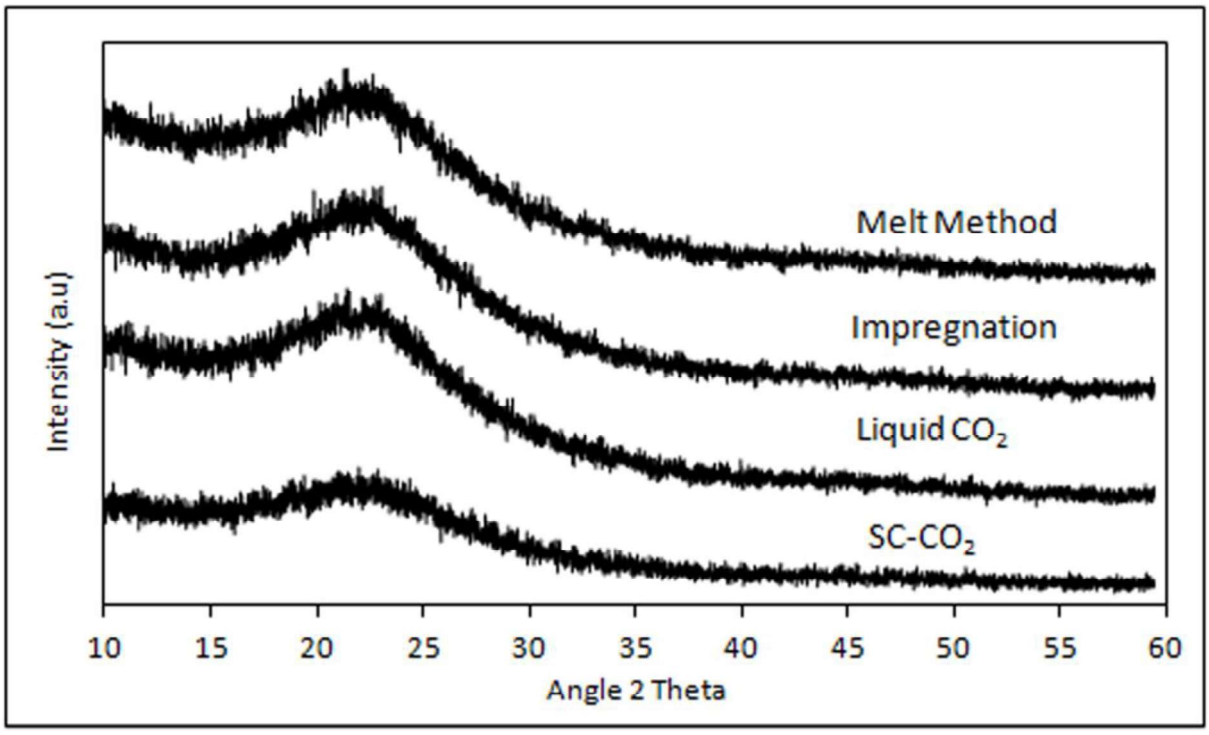

688

689 **Fig.6:** pXRD diffractograms of melt, impregnation, liquid and SC-CO_2 processed systems

690 post 12 month accelerated storage.

691

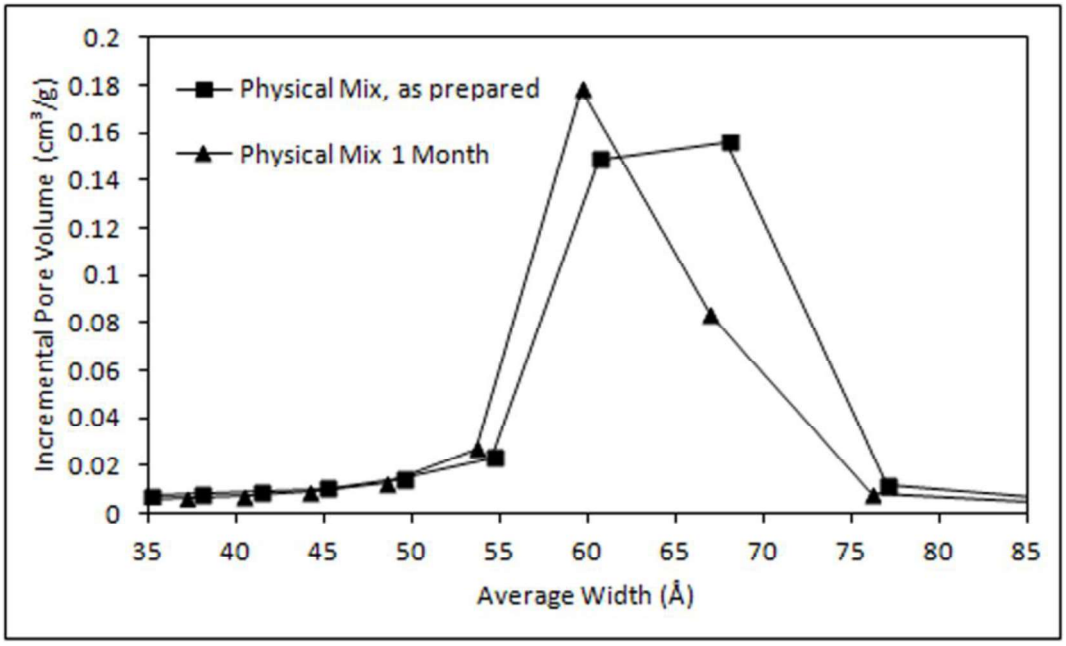

692

693 **Fig.7:** Pore size distribution of physical mix sample as prepared and after 1 month storage

694 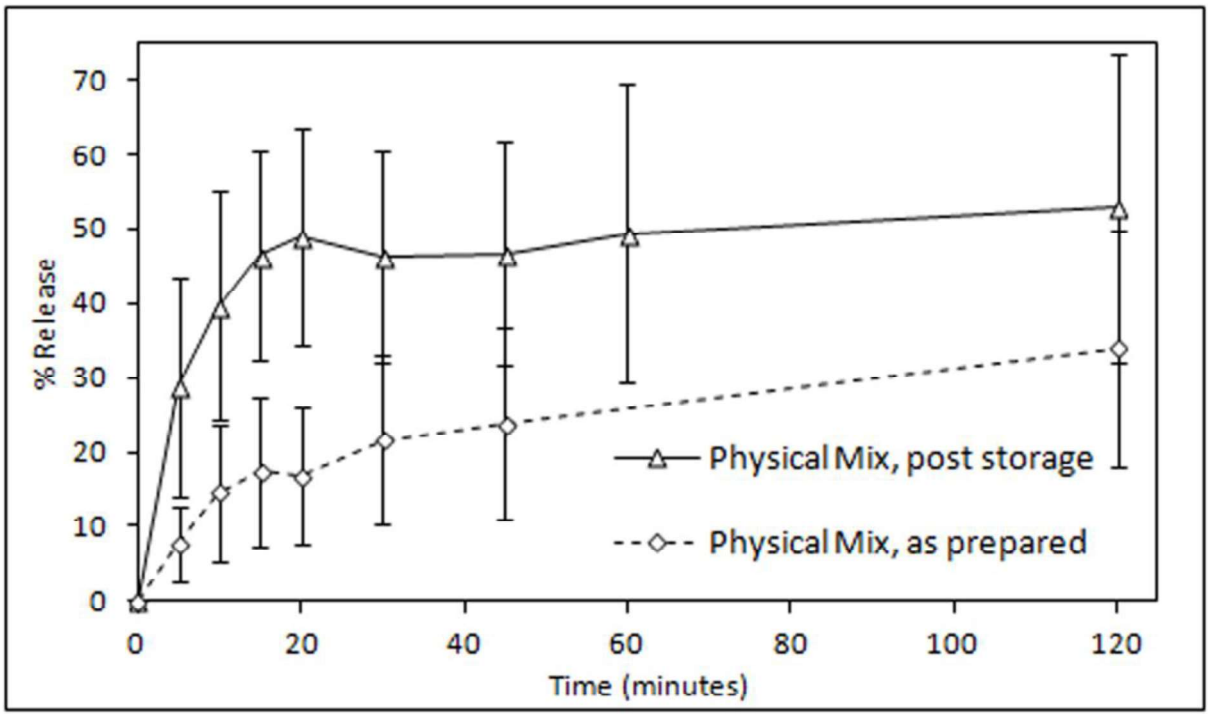

695 **Fig.8:** Release profile of physical mix sample as prepared and post 1 month storage

696

Figure(s)
Click here to download high resolution image

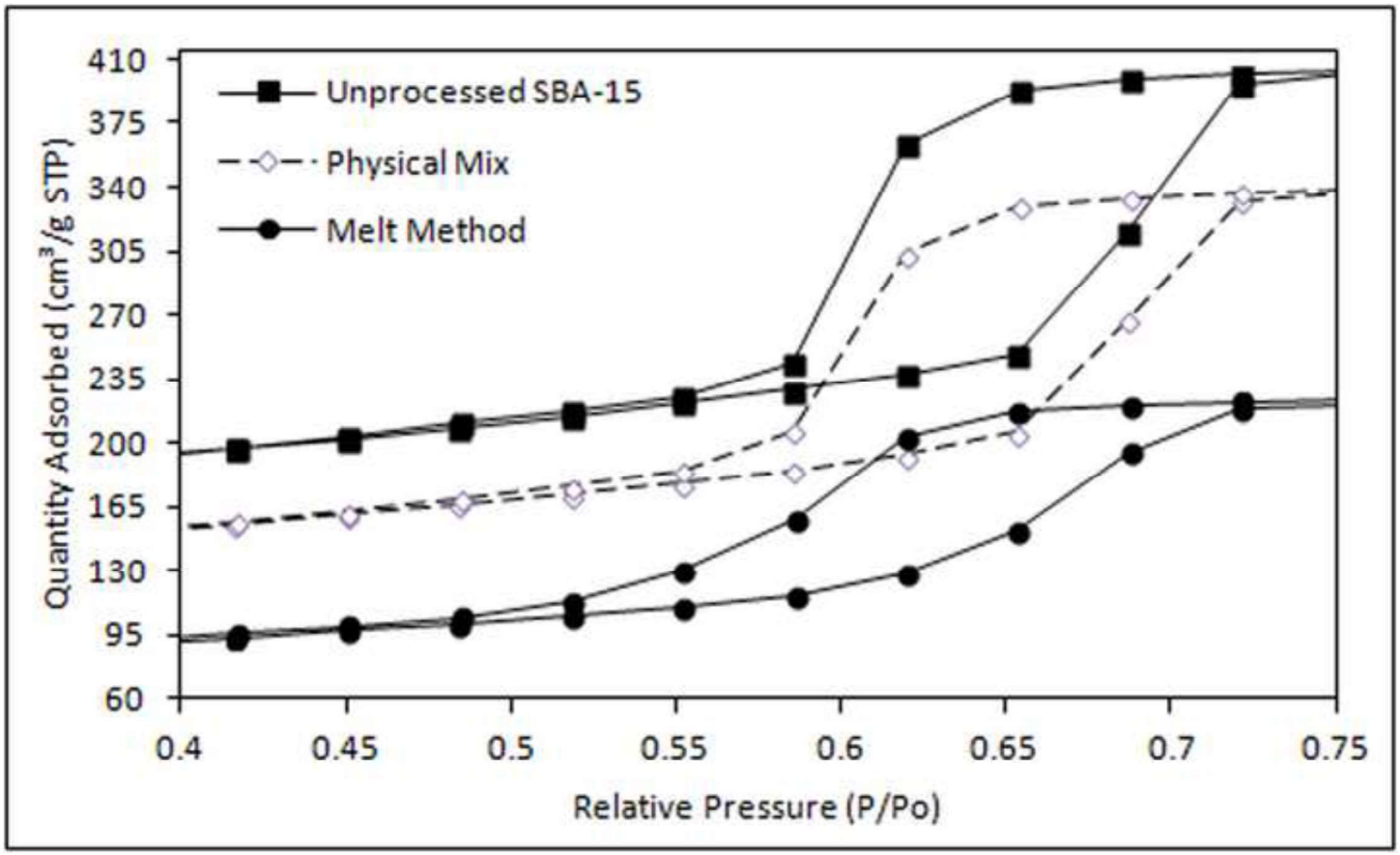

Figure(s)
Click here to download high resolution image

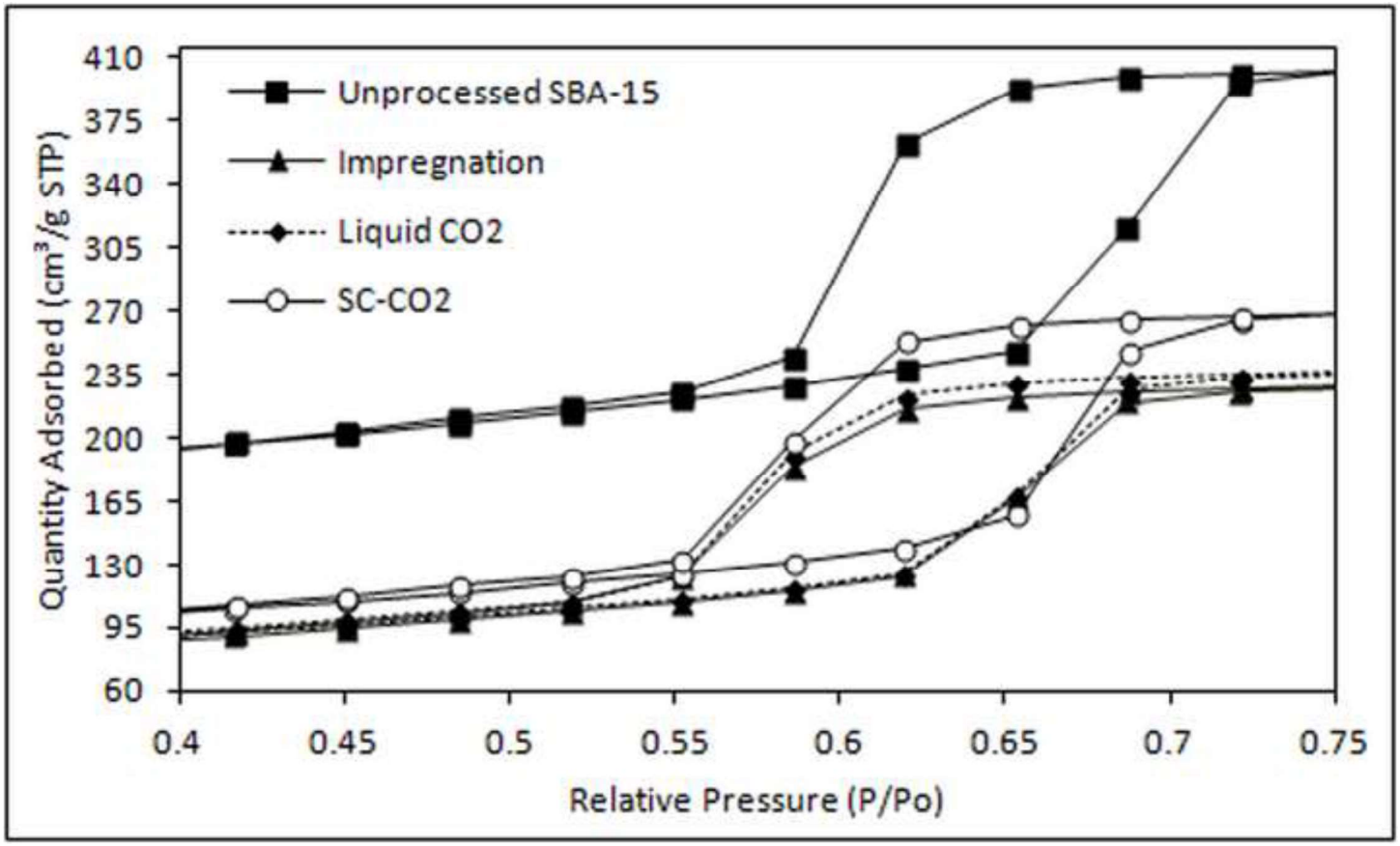

Figure(s)
Click here to download high resolution image

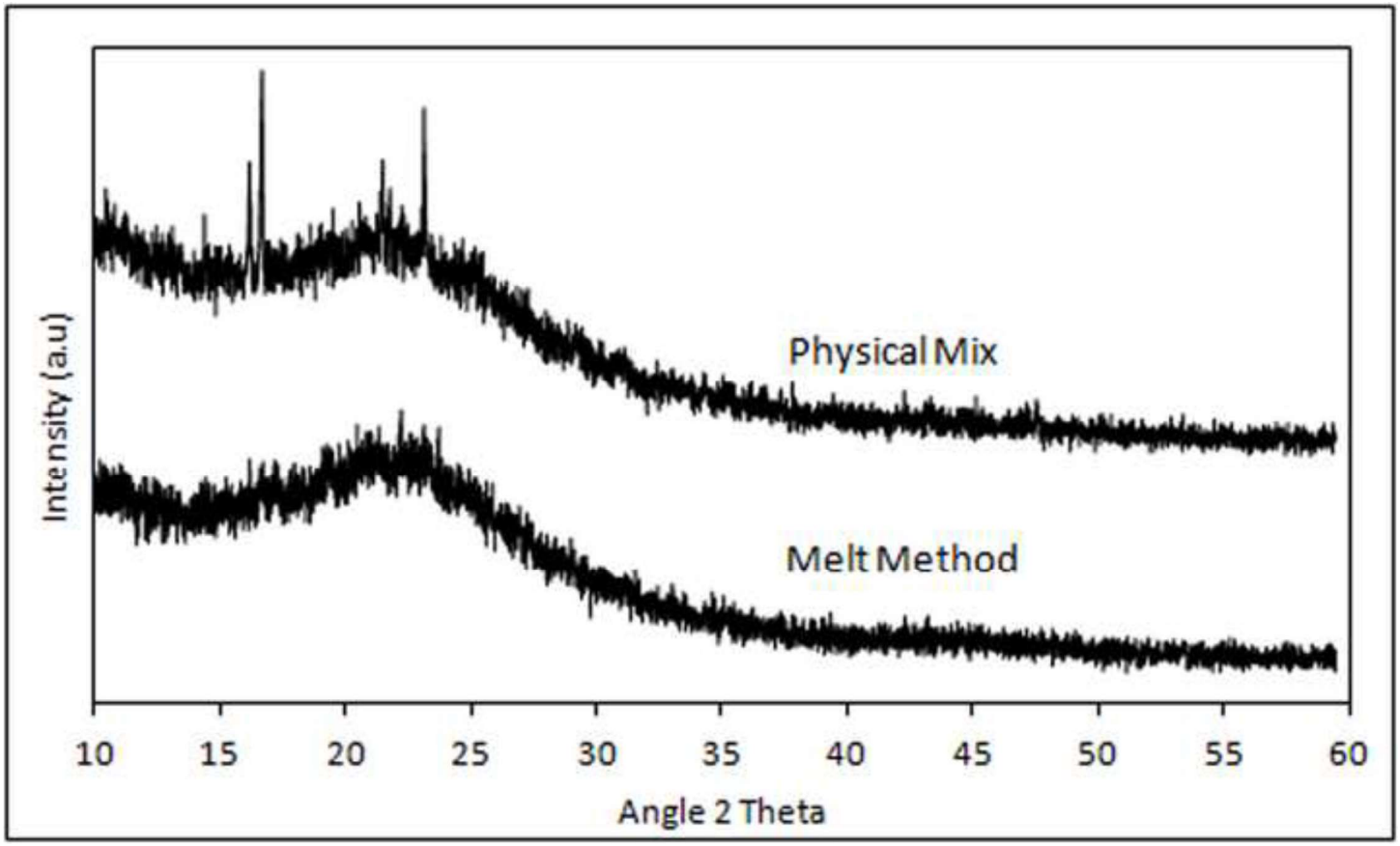

Figure(s)
Click here to download high resolution image

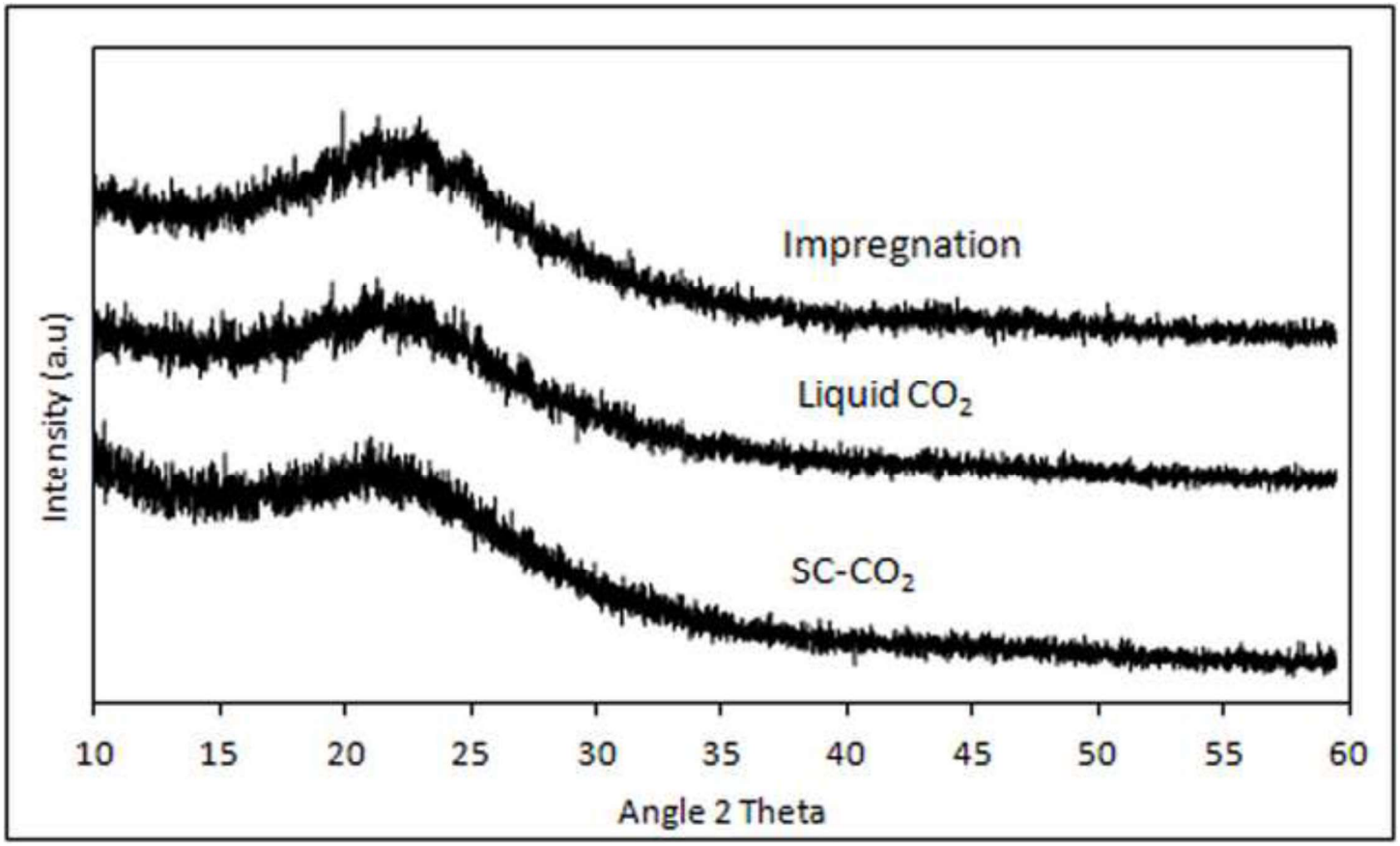

Figure(s)
Click here to download high resolution image

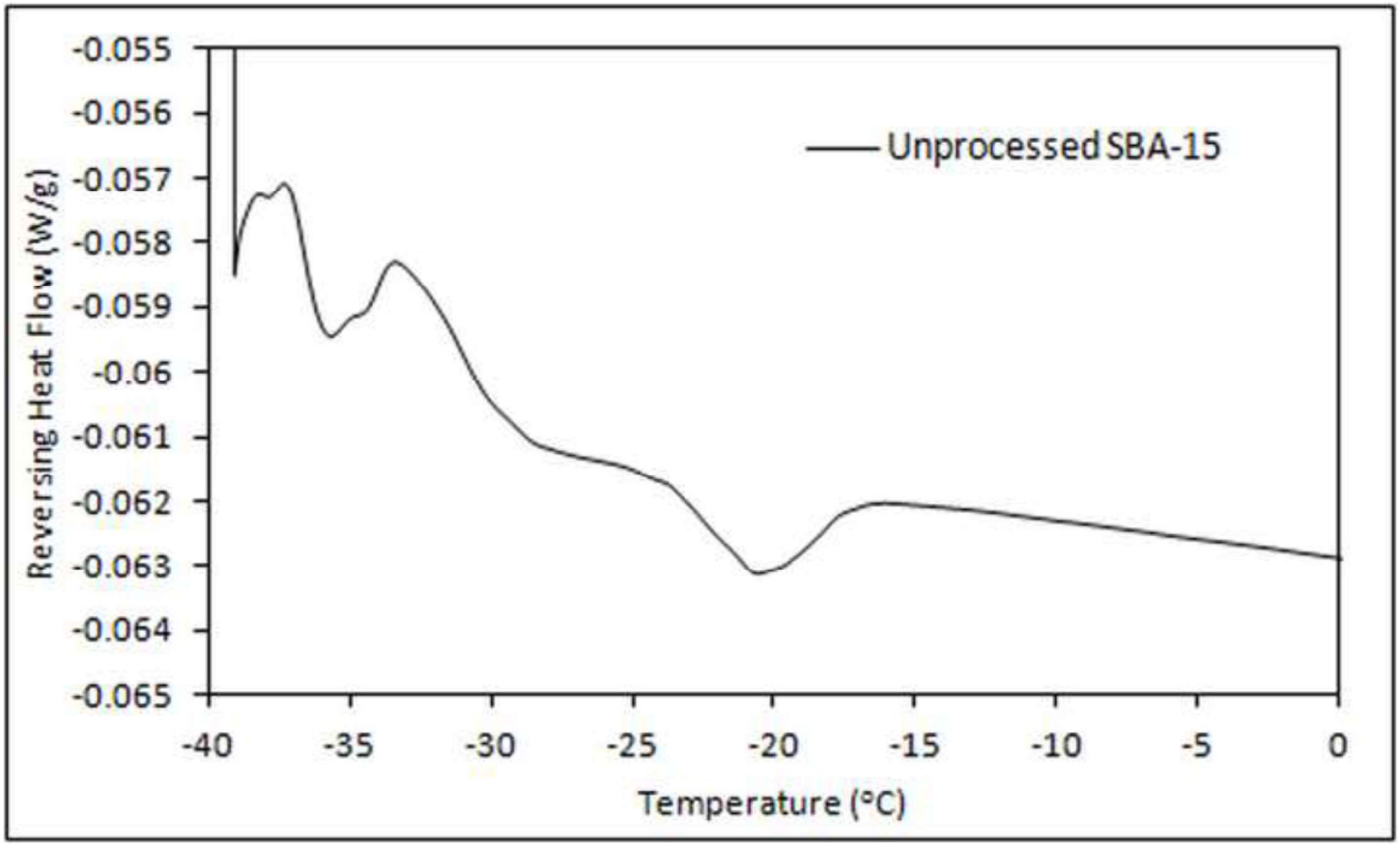

Figure(s)
Click here to download high resolution image

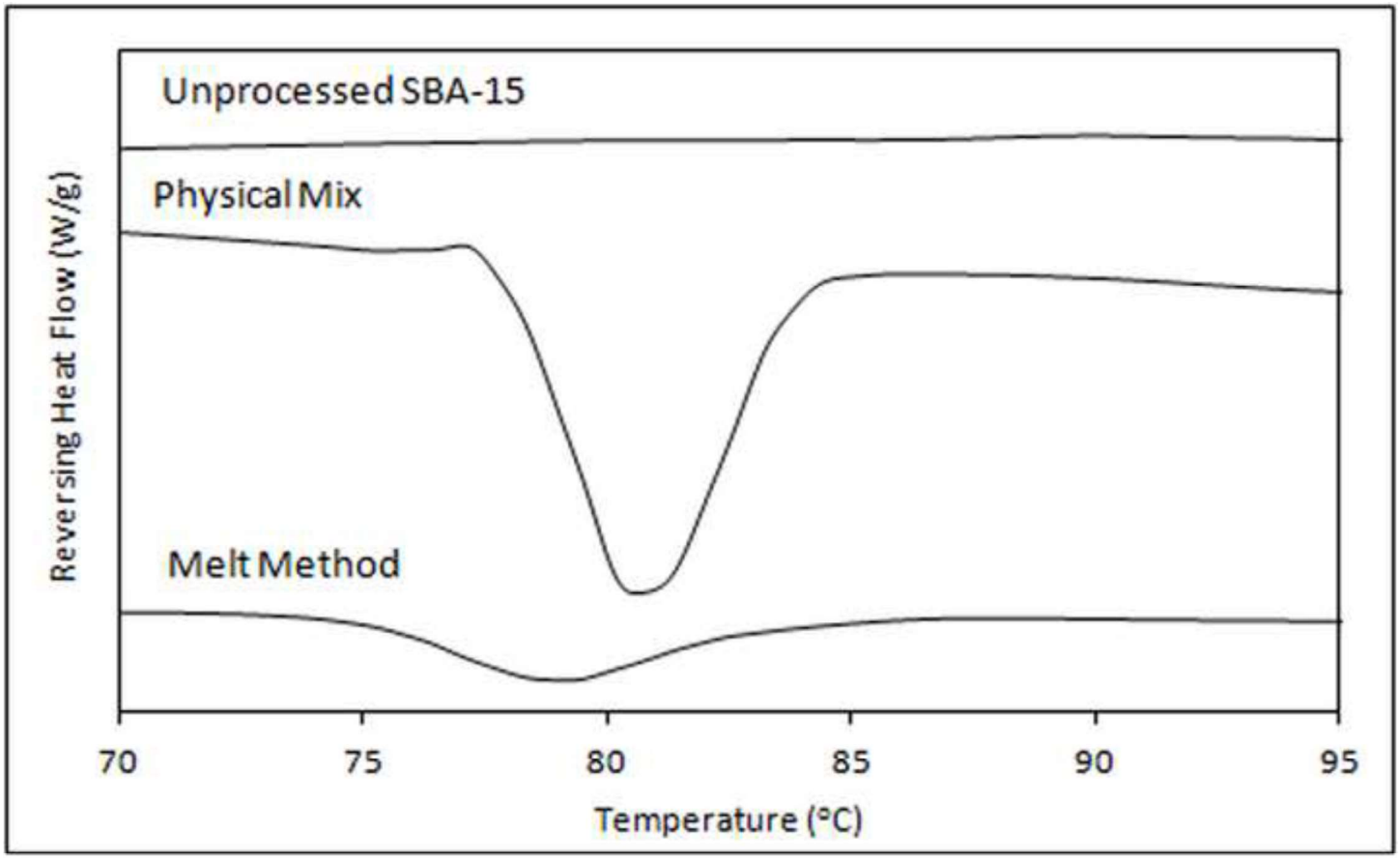

Figure(s)
Click here to download high resolution image

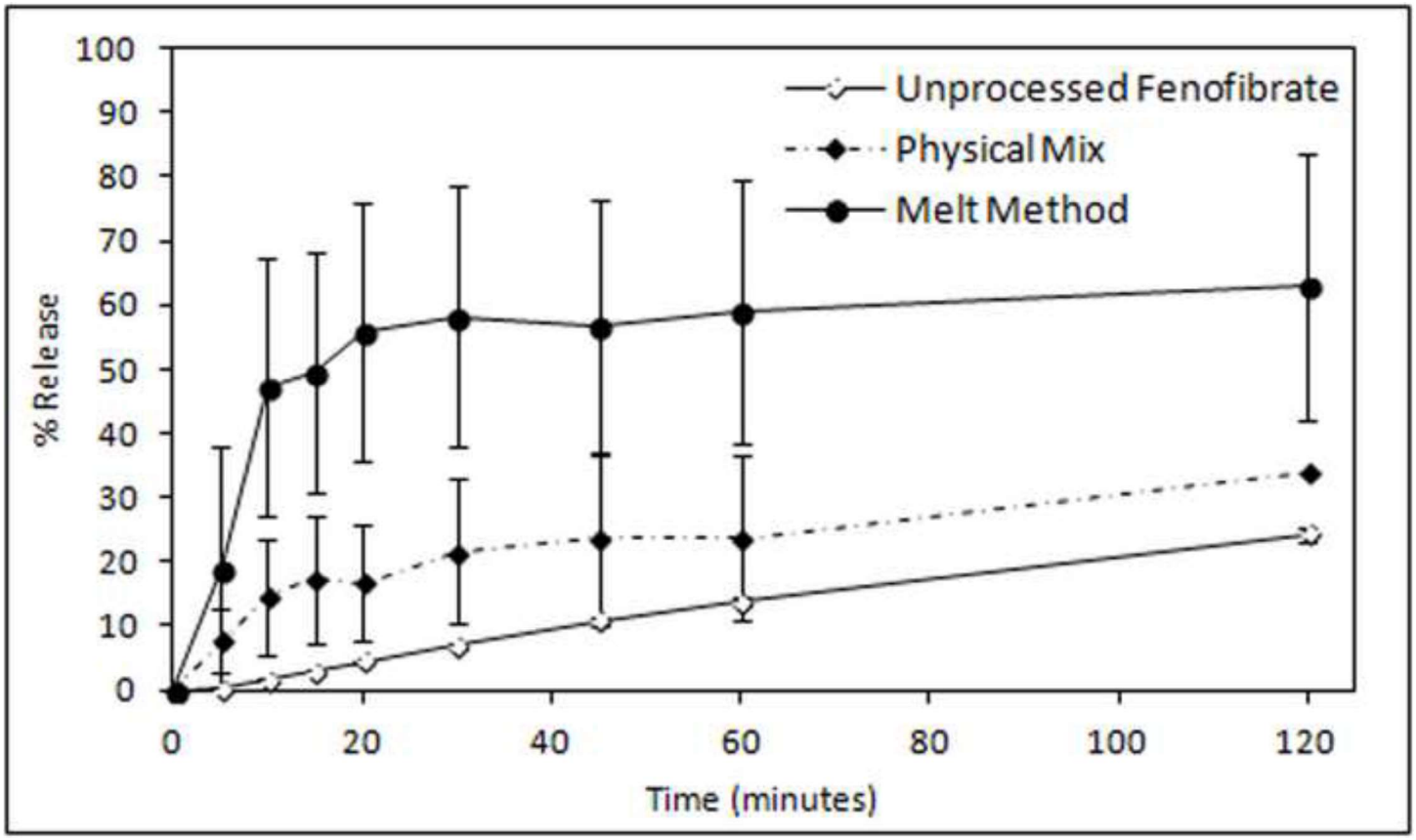

Figure(s)
Click here to download high resolution image

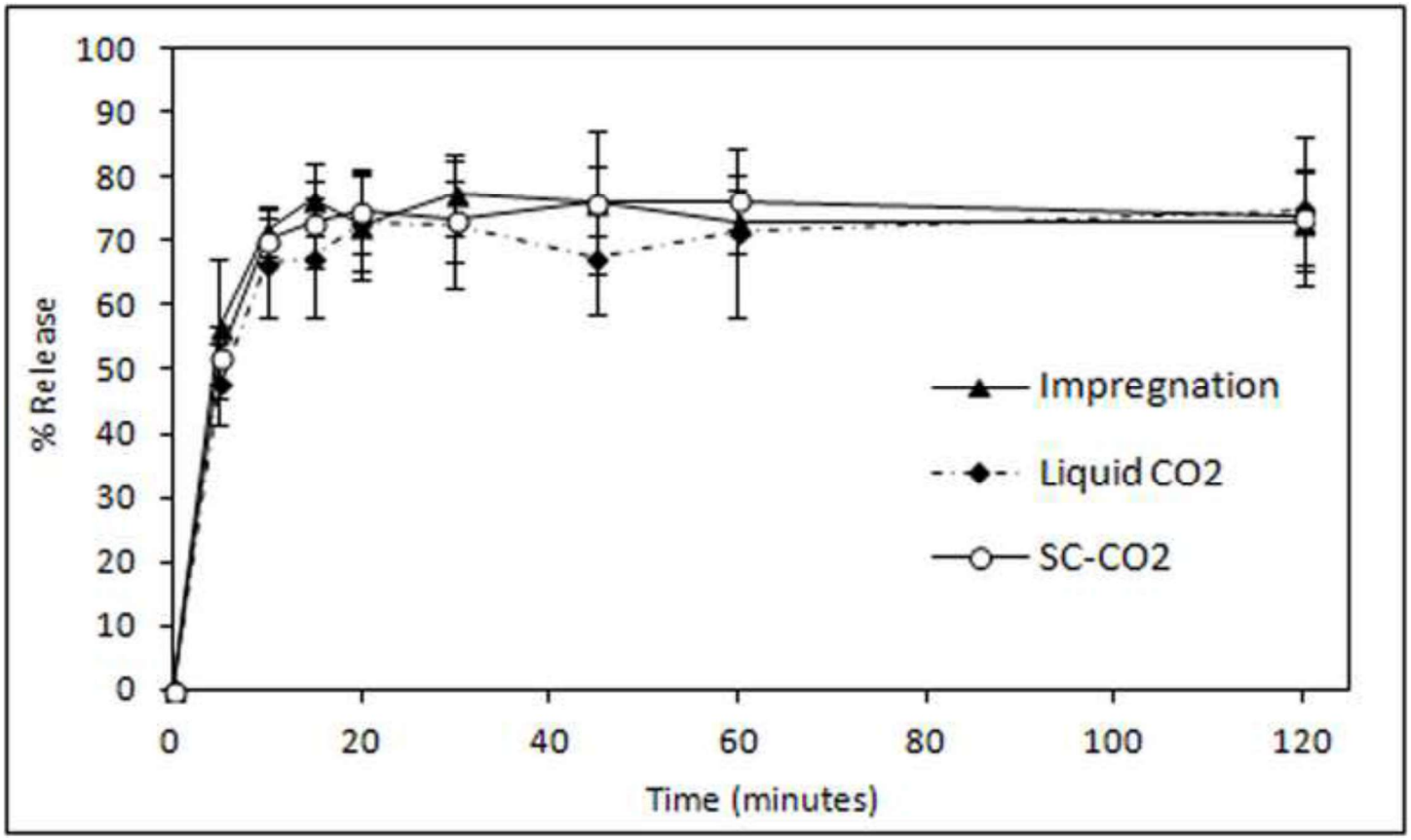

Figure(s)
Click here to download high resolution image

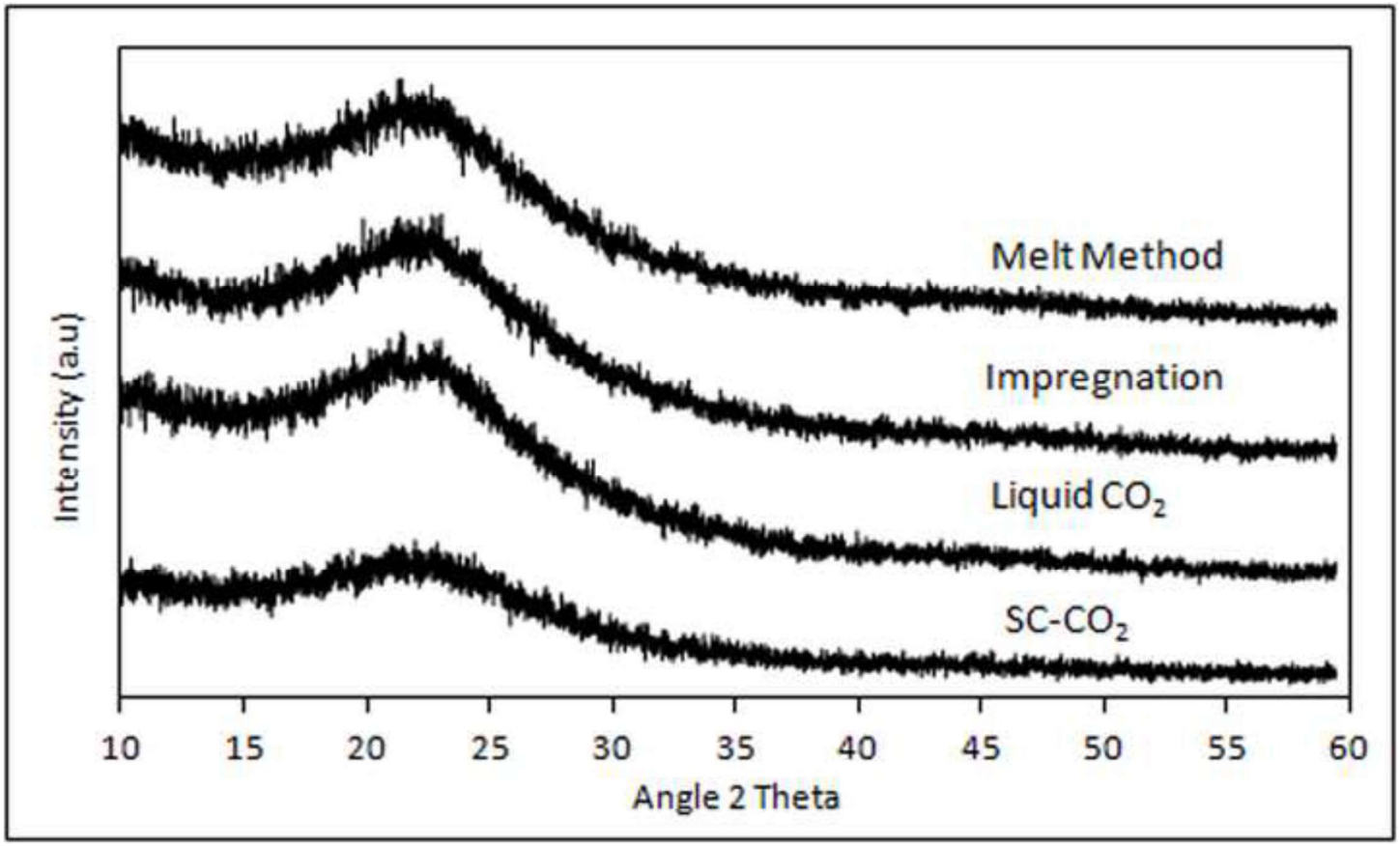

Figure(s)
Click here to download high resolution image

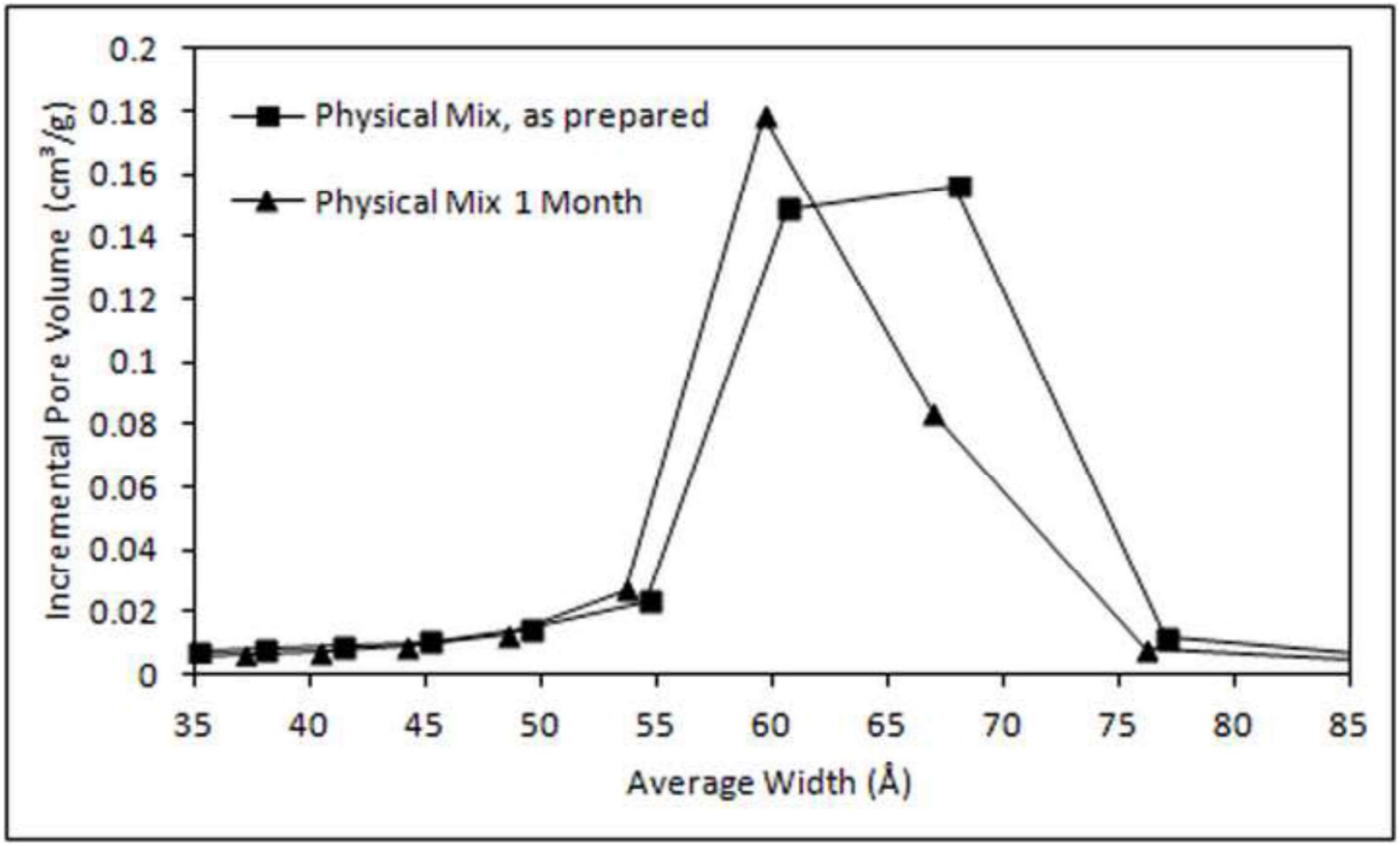

Figure(s)
Click here to download high resolution image